Original Article

Optical coherent tomography to evaluate the degree of inflammation in a mouse model of colitis

Jian Ding[1#], Jiewen Lin[2#], Qiu Li[1], Xiaoping Chen[3], Weiqiang Chen[2], Qiukun Zhang[2], Shanshan He[1], Ting Wu[1], Chengdang Wang[1], Shuncong Zhong[2], Dan Li[4]

[1]Digestive Department, the First Affiliated Hospital of Fujian Medical University, Fuzhou 350005, China; [2]Laboratory of Optics, Terahertz and Nondestructive Testing, School of Mechanical Engineering and Automation, Fuzhou University, Fuzhou 350108, China; [3]Department of Statistics, College of Mathematics and Informatics & FJKLMAA, Fujian Normal University, Fuzhou 350117, China; [4]Department of Gastroenterology, Union Hospital, Fujian Medical University, Fuzhou 350001, China

[#]These authors contributed equally to this work.

Correspondence to: Shuncong Zhong. Laboratory of Optics, Terahertz and Nondestructive Testing, School of Mechanical Engineering and Automation, Fuzhou University, Fuzhou 350108, China. Email: zhongshuncong@hotmail.com; Dan Li. Department of Gastroenterology, Union Hospital, Fujian Medical University, 29 Xinquan Road, Fuzhou 350001, China. Email: doctorlidan@163.com.

Background: There is an urgent need to develop a noninvasive imaging technique for the diagnosis of early inflammatory lesions or early and real-time microscopic assessment before selecting the most representative biopsy sites.

Methods: In this study, a dextran sulfate sodium colitis model was developed, and intestinal histological damage scores measured the degree of inflammation in colitis. According to these scores, 6 parameters were designed for hematoxylin and eosin (HE) sections based on morphological changes, and 2 parameters were designed for optical coherence tomography (OCT) images to measure submucosal edema by morphological changes to evaluate inflammation degrees in the colon. Spearman's rank correlation method was used to compare the correlation between the submucosal morphological changes and the different degrees of inflammation. One-way analysis of variance (ANOVA) was used for comparisons among groups, while receiver operating characteristic (ROC) curves of the indicators in HE sections and OCT images were plotted.

Results: In HE sections, angle of mucosal folds (r=0.853, P<0.01), length of basilar parts (r=0.915, P<0.01), submucosal area (r=0.819, P<0.01), and height between submucosal and muscular layers (r=0.451, P=0.001) were correlated with the degree of inflammation in colitis. In OCT images, length of basilar parts (r=0.800, P<0.01) and height of submucosa + thickness of muscularis (r=0.648, P=0.001) were correlated with the degree of inflammation and aided the measurement of inflammation in the colon.

Conclusions: Parameters based on morphological changes in OCT images and HE sections were significant indexes for evaluating the degree of inflammation in colitis. OCT images have advantages for future clinical applications in situ, including noninvasiveness and real-time imaging.

Keywords: Tomography, optical coherence; inflammation; colitis; inflammatory bowel disease; hematoxylin-eosin staining (HE staining)

Submitted Sep 27, 2019. Accepted for publication Mar 31, 2020.
doi: 10.21037/qims.2020.04.04
View this article at: http://dx.doi.org/10.21037/qims.2020.04.04

Introduction

Early damage of the gastrointestinal (GI) tract by inflammation manifests as hemodynamic changes, increased vascular permeability, and inflammatory exudation (1,2). These factors cause protein-rich fluid collection in the intestinal wall, especially in submucosal lesions. In Crohn's disease (CD), all layers of the intestinal wall are involved in inflammation, whereas in ulcerative colitis (UC), the mucosa and submucosa are mainly involved (3-6). In most cases, edema of the submucosa caused by inflammatory fluid collection is one of the most common early manifestations (6). Inflammation fluid is retained in the submucosal layer because of the laxity of the connective tissue in the submucosa. Thus, submucosal edema may be an independent marker for colorectal inflammation.

In both UC and CD, the typical disease course has recurrent flares and remissions (6). Disease extent and activity are commonly assessed clinically, endoscopically, and biochemically (7-11). Colonoscopy with biopsy is still the gold standard for assessment (10). However, evidence shows that microscopic inflammation can persist in the absence of clinical or endoscopic disease activity (11-13). Therefore, there is an urgent need to develop a noninvasive imaging technique for the diagnosis of early inflammatory lesions or early and real-time microscopic assessment prior to selecting the most representative biopsy sites.

In this study, we investigated the use of optical coherence tomography (OCT) to measure submucosal edema as a new noninvasive index to evaluate colorectal inflammation. We showed that OCT analysis of the intestinal wall had a strong correlation with histological anatomy, as shown in the mucosal layer (ultra-reflective layer) and the submucosal layer (low-reflective horizontal strip layer) (14). Therefore, OCT might be a noninvasive and convenient technique to measure early inflammation in colitis relapse. This study induced a DSS colitis model to examine morphological changes of the colorectal submucosa by OCT during inflammation to identify relevant diagnostic indexes for the diagnosis and classification of colorectal inflammation.

Methods

Animals and materials

Healthy female BALB/c mice (6–8 weeks of age, 18–22 g) were purchased from Wu's Laboratory Animal Center (Minhou County, Fuzhou, China). All animals were maintained under a 12 h light/dark cycle at 25 ℃ with a humidity of (60±10)% and were fed a standard diet *ad libitum*. Weight was recorded weekly. Animals in all groups had similar physiological parameters. All procedures involving experimental animals were conducted following protocols approved by the Institutional Animal Care and Use Committee (IACUC) of Fujian Medical University.

Induction of a DSS colitis model (15)

Mice were treated with 2.0%, 2.5%, or 3.0% dextran sodium sulfate (DSS) (MP Biomedicals; m.w. 36,000–50,000) in regular drinking water for 7 days. Mice were examined for changes in feces and weight loss on alternate days. Mice were sacrificed, then colons were harvested, flushed free of feces, and longitudinally slit open for further processing.

Histological scoring criteria and classifications for intestinal inflammation

The scoring criteria and classifications for intestinal inflammation are shown in *Tables 1* and *2* (15,16).

OCT (17)

The GAN210C1 spectral-domain OCT system (center wavelength, 930 nm; axial resolution, 6 μm; a-scan line rat, 5.5–36 kHz) was used for this experiment. The output of

Table 1 Histological scoring criteria for intestinal inflammation (15,16)

Score	Neutrophil grade	Lesion depth	Crypt destruction	Lesion range
0	0/high magnification	Nil	Nil	0
1	<10/high magnification	Mucosa	Basal 1/3 damage	1–25%
2	10–50/high magnification	Submucosa	Basal 2/3 damage	26–50%
3	>50/high magnification	Muscularis	Only surface epithelium intact	51–75%
4	Visible acute inflammation with ulceration	Serosa	Entire crypt and epithelium lost	76–100%

FC/APC fibers with a central wavelength of 850–1,000 nm was collimated and routed to the beam splitter cube. The beams were divided into sample beams and reference beams similar to the Michelson interferometer. Sample beams were routed through mirrors driven by 2 galvanometers to allow for scanning on 2 axes. Subsequently, the scanning target focused the beam on samples. Backscattered and reflected light were collected and propagated back to the optical fiber by the scanning objectives. The light reflected in the reference arm was reflected into the optical fiber. For reference light, the optimum intensity was adjusted using a knob, which opened or closed the variable aperture of the OCT. Spectral domain OCT (SD-OCT) is an imaging modality that provides cross-sectional images with micrometer resolution that are generated by the interference between a reference optical path which is reflected from the eye. The SD-OCT system employs a broadband light source with a spectrometer for detection. The phase delay of back reflection and backscattered light (relative to a stationary reference) is recorded as a function of wavenumber, and the fast Fourier transform (FFT) generates cross-sectional images as a function of sample depth (*Figure 1*; Optical Layout OCT Common-Path in https://www.thorlabschina.cn/).

Table 2 Classifications for intestinal inflammation (15,16)

Degree of inflammation	Normal	Mild	Moderate	Severe
Score	0–3	4–6	7–10	11–14

OCT imaging procedure

All image analyses using OCT were carried out using custom routines written in Matlab. The sections were analyzed under a light microscope (Olympus CX41), and quantitative data were analyzed by Image-Pro Plus 6.0.0260 (*Figure 2*).

Mice with DSS-induced colitis fasted for 12 h for solid food and 6 h for water and then were sacrificed by inhalation anesthesia with isoflurane. Colons were removed, and colorectal tissues 2 cm from the anal margin with a length of 0.5 cm were removed, cut open lengthwise, rinsed with saline, and laid on glass slides after drying on filter paper. Samples were placed in the scanning window for OCT scanning (*Figure 3*).

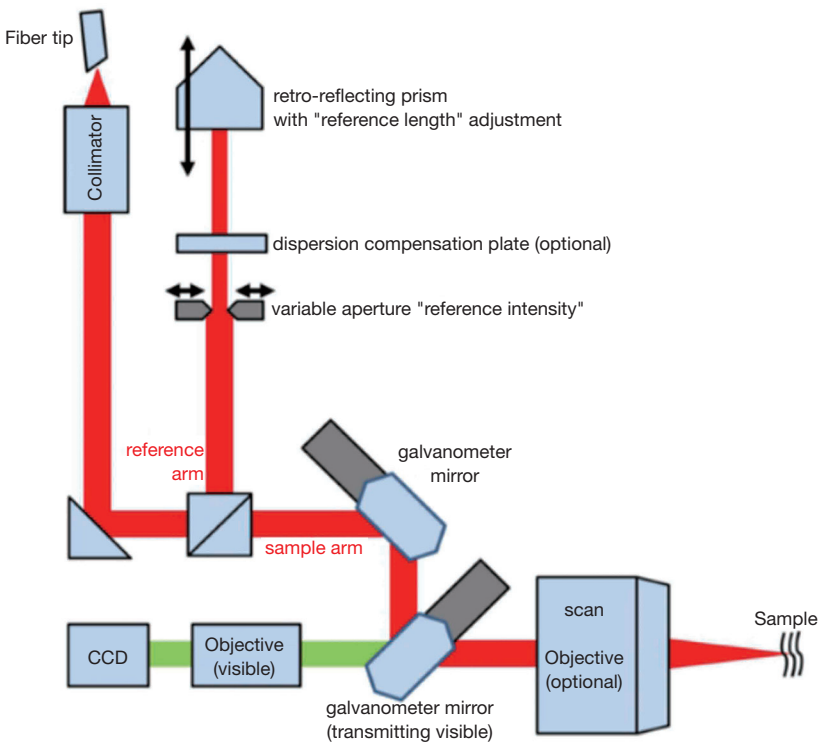

Figure 1 Optical layout OCT common path (https://www.thorlabschina.cn/). OCT, optical coherent tomography.

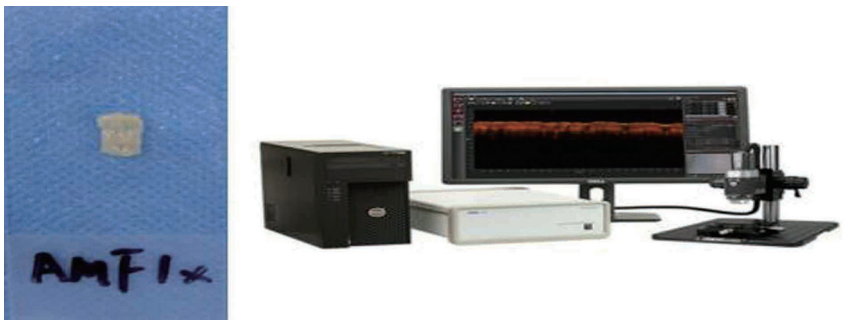

Figure 2 Colorectal tissue for scanning (right); OCT scan system (https://www.thorlabs.com/). OCT, optical coherent tomography.

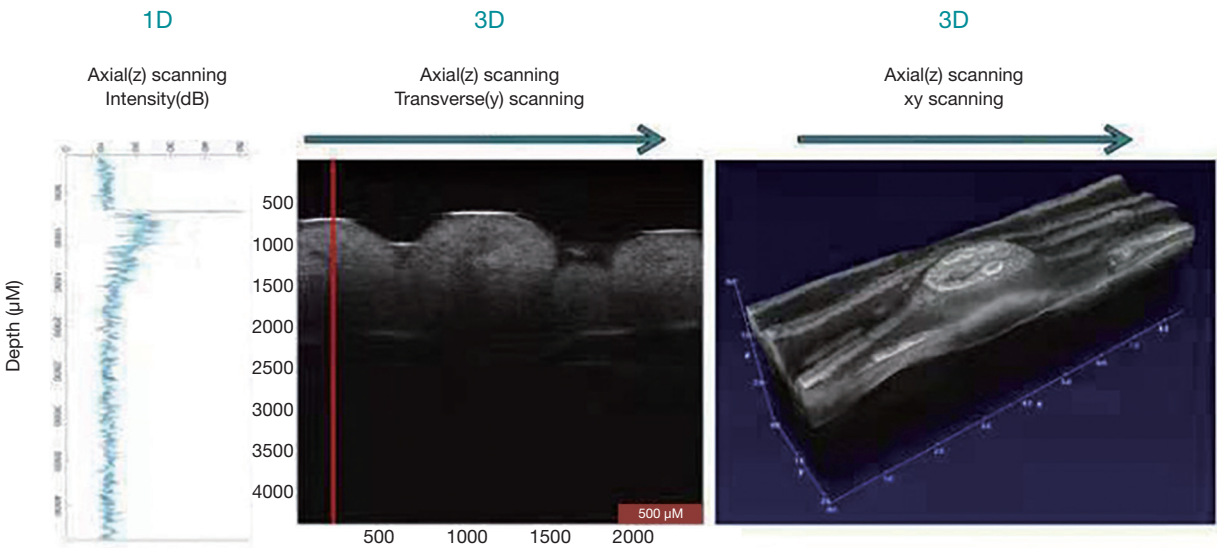

Figure 3 The entire 3D imaging process of OCT. OCT, optical coherent tomography.

Histologic analysis

After collecting OCT data, tissue samples were fixed with 4% paraformaldehyde for 24 h. Subsequently, the tissue blocks were dehydrated, made transparent, dipped in wax, embedded in paraffin blocks, cut into 4 μm sections, and then stained by hematoxylin and eosin (HE). The images were examined and captured by another group of experienced histology researchers in a blinded manner using a microscope.

Data analysis

Spearman's rank correlation method was used to compare the correlation between the submucosal morphological changes and the different degrees of inflammation. The larger the absolute value of the coefficient, the stronger the correlation between the variables. Measurement data were represented as the mean ± SD, and one-way analysis of variance (ANOVA) was used for comparisons among groups. In line with the homogeneity of variance, the least significance difference (LSD) method was used when assuming homogeneity of variance. If the homogeneity of variance was not satisfied, the Games-Howell (A) method (applicable to non-assumed homogeneity of variance) was used. $P<0.05$ was considered statistically significant. Receiver operating characteristic (ROC) curves of the indicators in HE staining and OCT images were plotted. A ROC curve closer to the upper left corner indicated a higher overall accuracy of the test.

Table 3 Numbers of acquired OCT images and HE-stained sections

Groups	Mice	HE-stained sections	OCT images
Controls	12	12	3,996
DSS colitis models	40	40	13,320

OCT, optical coherent tomography; DSS, dextran sodium sulphate; HE, hematoxylin and eosin.

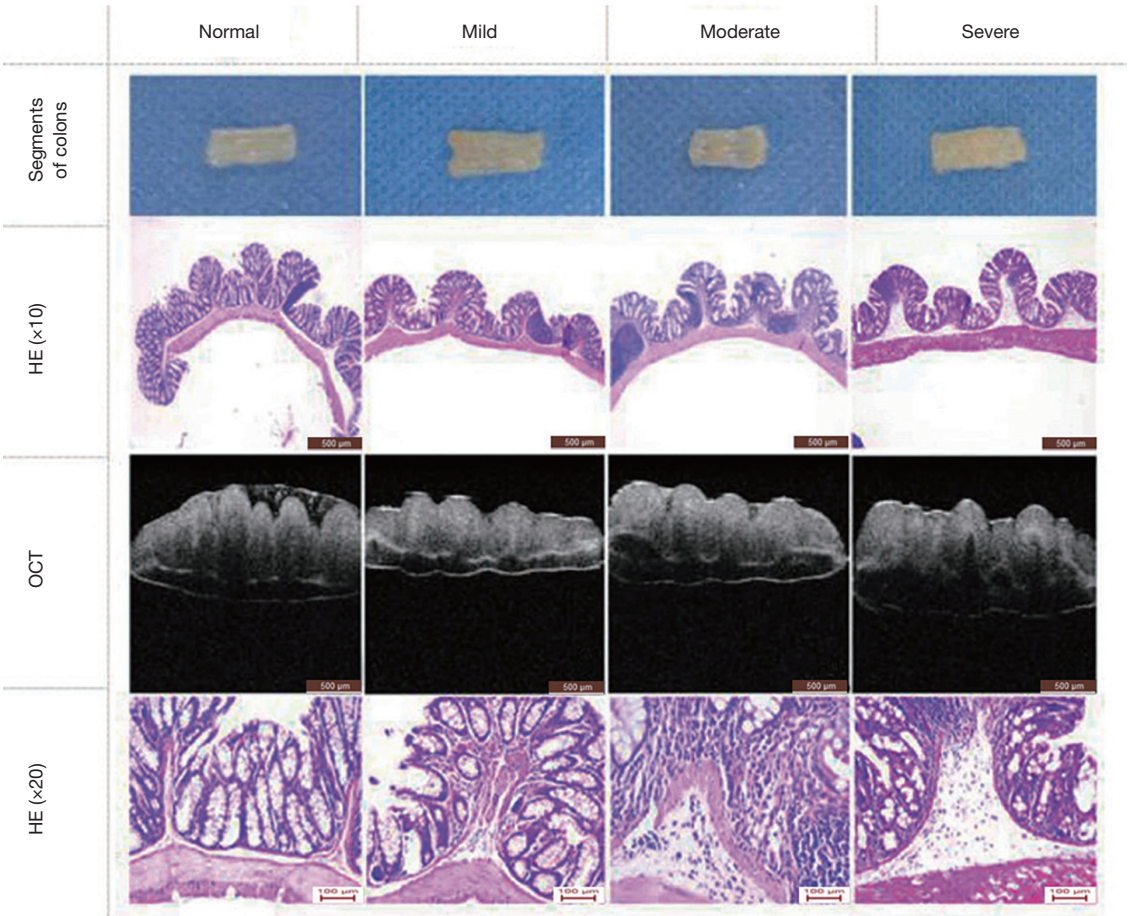

Figure 4 According to the morphological and structural characteristics of the HE-stained pathological section, the corresponding OCT images were matched. OCT, optical coherent tomography.

Results

OCT images and HE-stained sections for DSS-induced colitis in mice

Mice orally administered with DSS were induced to develop acute colitis successfully. Two mice died after taking 3% DSS for 10 days. OCT images and HE-stained sections were acquired (*Table 3*). A comparison of OCT images and HE stained sections are shown in *Figure 4*. OCT images and HE-stained pathological sections were matched according to the morphological and structural characteristics.

Results of intestinal histological damage scores in a DSS colitis mouse model

According to the histological scoring criteria for colitis damage, the degree of inflammatory infiltration is classified into 4 grades: normal, mild, moderate, and severe (*Figure 5*).

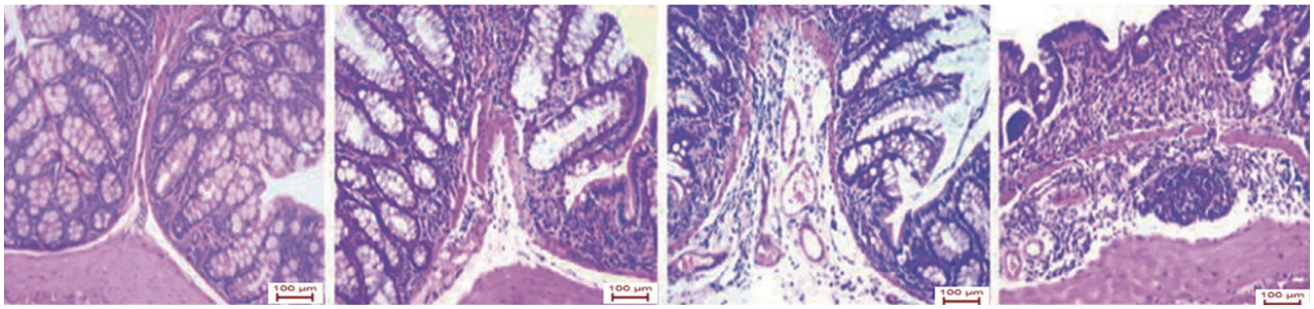

Figure 5 According to histological scoring criteria for colitis damage, degrees of inflammatory infiltration were classified into 4 grades in HE sections: normal, mild, moderate, and severe.

Table 4 Classifications and numbers of DSS-induced mouse models in different histological damage degrees

Degree of inflammation	Normal	Mild	Moderate	Severe
Scores	0–3	4–6	7–10	11–14
Numbers	12	10	11	19

DSS, dextran sodium sulphate.

Mouse models were classified into different groups based on scores acquired with the HE-stained sections (*Table 4*).

Definition of parameters for indexes of colorectal inflammation in HE-stained pathological sections

We defined 6 candidate parameters to measure the submucosal edema induced by inflammation in HE stained sections: (a) angle of mucosal folds (°), the apex of the angle is the highest point of the mucosal wrinkle, with 2 straight lines from the angle being placed along both sides of the mucosal muscular layers; (b) length of submucosal basilar part (μm), the distance between the 2 lower points of the mucosal muscularis; (c) area of submucosa (μm^2), area of the submucosal layer in the mucosa wrinkle; (d) height of submucosa (μm), the distance from the lower end of the mucosal muscularis to the upper end of the muscularis; (e) thickness of muscularis (μm), the distance from the upper end to the lower end of the muscularis; (d+e) height of submucosa + thickness of muscularis (μm) (*Figures 6*,*7*). The parameters were measured in each HE stained sections, and the mean value was determined.

Definitions of parameters for indexes of colorectal inflammation in OCT images

We defined 2 candidate parameters to measure submucosal edema induced by inflammation in OCT images: (f) length of basilar part, the distance between the 2 lower points of the mucosal muscularis; (g) height of submucosa + thickness of muscularis (μm), distance from the upper end of the submucosal layer to the lower end of the muscularis (*Figure 7*).

Statistical analysis

Spearman's rank correlation test of parameters as indexes of colorectal inflammation in HE-stained pathological sections

The correlation coefficients were analyzed between the angle of mucosal folds and the degree of inflammation ($r=0.853$, $P<0.01$), between the length of basilar parts and the degree of inflammation ($r=0.915$, $P<0.01$), between the area of submucosa and the degree of inflammation ($r=0.819$, $P<0.01$), between the height of submucosa and the degree of inflammation ($r=0.451$, $P=0.001$); all were found to be statistically significant; however, the correlation coefficients between the muscle layer thickness and the degree of inflammation ($r=-0.093$, $P>0.05$), and between height of submucosa + thickness of muscularis and the degree of inflammation ($r=0.209$, $P>0.05$), were not found to be statistically significant (*Table 5*).

Analysis of significance between different groups by mean ± standard deviation and single-factor variance in HE-stained pathological sections

The angle between mucosal folds increased gradually with an increase in the degree of inflammation. There were significant differences when the normal group was compared with the moderate and severe groups, and when the mild group was compared with the moderate and severe groups ($P<0.05$). The length of basilar parts increased

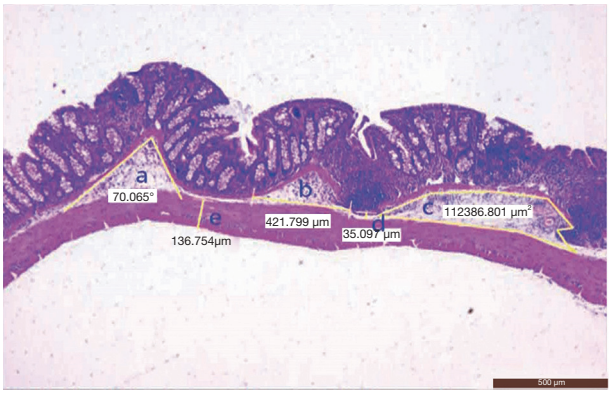

Figure 6 We defined 6 candidate variables to measure the submucosal edema induced by inflammation in HE stained sections: (a) angle of mucosal folds (°); (b) length of basilar part (μm); (c) area of submucosa (μm²); (d) height of submucosa (μm); (e) thickness of muscularis (μm); (d+e) height of submucosa + thickness of muscularis (μm).

gradually with an increase in the degree of inflammation, which was statistically significant between any 2 parameters (P<0.05). The area of submucosa increased with an increase in the degree of inflammation, and statistical significance was observed when the normal group was compared with the moderate and severe groups, when the mild group was compared with the severe group, and when the moderate group was compared with the severe group (P<0.05). Height of submucosa increased gradually with an increase in the degree of inflammation, and statistical significance was observed when the normal group was compared with the severe group, when the mild group was compared with the severe group, and when the moderate group was compared with the severe group (P<0.05). There were no correlations between the degree of inflammation and thickness of muscularis or the height of the submucosa + thickness of

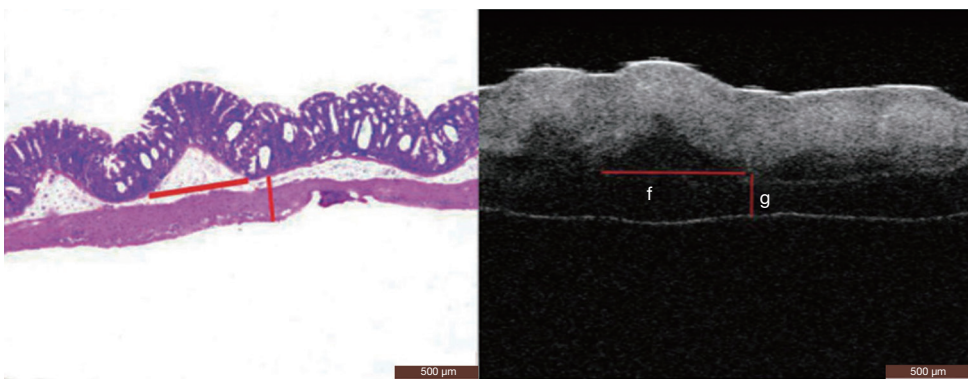

Figure 7 We defined 2 candidate parameters to measure submucosal edema induced by inflammation in OCT images: (f) Length of basilar part; (g) height of submucosa + thickness of muscularis (μm). And the corresponding HE sections were matched.

Table 5 Spearman's rank correlation test for parameters for indexes of colorectal inflammation in HE-stained pathological sections

		The angle of mucosal folds (°)	Length of the basilar part (μm)	Area of the submucosa (μm²)	Height of submucosa (μm)	The thickness of muscularis (μm)	Height of submucosa + thickness of muscularis (μm)
Inflammation degree in HE	r	0.853	0.915	0.819	0.451	–0.093	0.209
	Sig. (double test)	0.000	0.000	0.000	0.001	0.510	0.137
	N	52	52	52	52	52	52

The correlation is significant with a confidence level (double test) of 0.01.

Table 6 Analysis of significance between different groups by mean ± standard deviation and single-factor variance in HE-stained pathological sections

Dependent variables	Degree of inflammation	Numbers of HE	Mean ± standard deviation	P values		
				Mild	Moderate	Severe
Angle of mucosal folds (°)	Normal	12	9.26±3.26	0.154	0.000	0.000
	Mild	10	16.92±10.01		0.001	0.000
	Moderate	11	63.35±27.04			0.129
	Severe	19	89.80±36.01			
Length of basilar part (μm)	Normal	12	55.48±15.68	0.014	0.000	0.000
	Mild	10	88.45±25.43		0.005	0.000
	Moderate	11	157.09±49.55			0.000
	Severe	19	349.55±159.29			
Area of submucosa (μm^2)	Normal	12	11,917.70±4,021.05	0.067	0.003	0.000
	Mild	10	18,734.04±6,937.69		0.545	0.000
	Moderate	11	23,051.86±7,732.64			0.000
	Severe	19	54,115.23±25,978.43			
Height of submucosa (μm)	Normal	12	26.87±7.55	0.936	0.953	0.005
	Mild	10	24.89±8.24		1.000	0.003
	Moderate	11	25.19±7.88			0.002
	Severe	19	39.70±11.88			
Thickness of muscularis (μm)	Normal	12	120.23±15.42	0.294	0.511	0.702
	Mild	10	127.54±13.78		0.101	0.134
	Moderate	11	115.79±13.37			0.724
	Severe	19	117.95±18.71			
Height of submucosa + thickness of muscularis (μm)	Normal	12	147.10±19.14	0.517	0.445	0.140
	Mild	10	152.42±17.55		0.176	0.486
	Moderate	11	140.98±16.12			0.025
	Severe	19	157.65±21.10			

The significance level is set at α =0.05, and differences are significant when P<0.05.

muscularis. Only the difference in the height of submucosa + thickness of muscularis between the moderate and severe groups was statistically significant (P<0.05) (*Table 6*).

Spearman's rank correlation test of parameters for indexes of colorectal inflammation in OCT images

The correlation coefficient between the length of basilar parts and the degree of inflammation was 0.800 (P<0.01), while that between the height of submucosa + thickness of muscularis and the degree of inflammation was 0.648 (P=0.001); both were statistically significant (*Table 7*).

Analysis of significance between different groups by the mean ± standard deviation and single-factor variance in OCT images

The length of basilar parts increased gradually with an

Table 7 Spearman's rank correlation between inflammation degree and 2 candidate variables of OCT

		Length of the basilar part (μm)	Height of submucosa + thickness of muscularis (μm)
Inflammation degree in HE	r	0.800	0.648
	Sig. (double test)	0.000	0.001
	N	52	52

The correlation is significant with a confidence level (double test) of 0.01. (f) Length of basilar part; (g) height of submucosa + thickness of muscularis (μm). OCT, optical coherent tomography.

Table 8 Analysis of significance between different groups by mean comparison and one-way ANOVA in HE-stained pathological sections

Dependent variables	Degree of inflammation	Numbers of HE	Mean ± standard deviation	P values		
				Mild	Moderate	Severe
Length of basilar part (px)	Normal	12	215.97±84.82	0.393	0.000	0.000
	Mild	10	317.73±108.08		0.047	0.000
	Moderate	11	517.55±130.60			0.024
	Severe	19	743.86±273.49			
Height of submucosa + thickness of muscularis (px)	Normal	16	277.74±43.54	0.336	0.158	0.000
	Mild	6	259.27±42.33		0.025	0.000
	Moderate	11	304.31±60.95			0.006
	Severe	19	352.27±33.79			

The significance level is set at α =0.05, and the differences are significant when P<0.05. ANOVA, one-way analysis of variance; HE, hematoxylin and eosin.

increase in the degree of inflammation, and statistical significance was observed when the normal group was compared with the moderate and severe groups, the mild group was compared with the severe group, and the moderate group was compared with the severe group (P<0.05). Height of submucosa + thickness of muscularis increased gradually with an increase in the degree of inflammation, and statistical significance was observed when the normal group was compared with the severe group, the mild group was compared with the moderate and severe groups, and the moderate group was compared with the severe group (P<0.05) (*Table 8*).

ROC curves

To determine the diagnostic power of these indicators for evaluating colorectal inflammation, we respectively plotted the ROC curves of these indicators in HE-stained pathological sections and OCT images. As shown in *Table 9* and *Figure 8*, according to the order, the area under ROC curve of 6 parameters designed for HE sections were 0.933 (P=0.000), 0.973 (P=0.000), 0.930 (P=0.000), 0.617 (P=0.224), 0.517 (P=0.862), and 0.581 (P=0.397), respectively. The area under the ROC curve of 2 parameters designed for OCT images was 0.922 (P=0.000) and 0.699 (P=0.038), respectively (*Table 10* and *Figure 9*).

Discussion

Optical coherent tomography (OCT) is a powerful noninvasive optical imaging technology (14,17-20) that provides a cross-sectional image or 3D imaging of tissues with low-energy infrared light (14,17,18). The imaging-forming principle is similar to ultrasound, but it uses near-infrared light at wavelengths of 750–1,300 nm instead of sound waves, resulting in a higher axial resolution less than 10 μm, 10–25 times finer than that of ultrasound (14,17-20). OCT imaging requires no coupling media, can be imaged in water or air directly, and can be performed close to the histopathological structure (17). The imaging depth of OCT is 2–3 mm (14,17,20), which is sufficient to image

Table 9 ROC curves of parameters for indexes of colorectal inflammation in HE sections

Parameters for indexes of colorectal inflammation	Area[#]	Standard error	Asymptotic Sig.	Asymptotically 95% confidence interval	
				Lower bound	Upper bound
The angle of mucosal folds (°)	0.933	0.035	0.000	0.865	1.000
The length of basilar parts (μm)	0.973	0.021	0.000	0.932	1.000
The area of submucosa (μm^2)	0.930	0.035	0.000	0.861	0.999
The height of submucosa (μm)	0.617	0.086	0.224	0.449	0.784
The muscle layer thickness (μm)	0.517	0.095	0.862	0.331	0.702
Height of submucosa + thickness of muscularis (μm)	0.581	0.092	0.397	0.401	0.762

[#] the area under the ROC curve. OCT, optical coherent tomography; ROC, receiver operating characteristic.

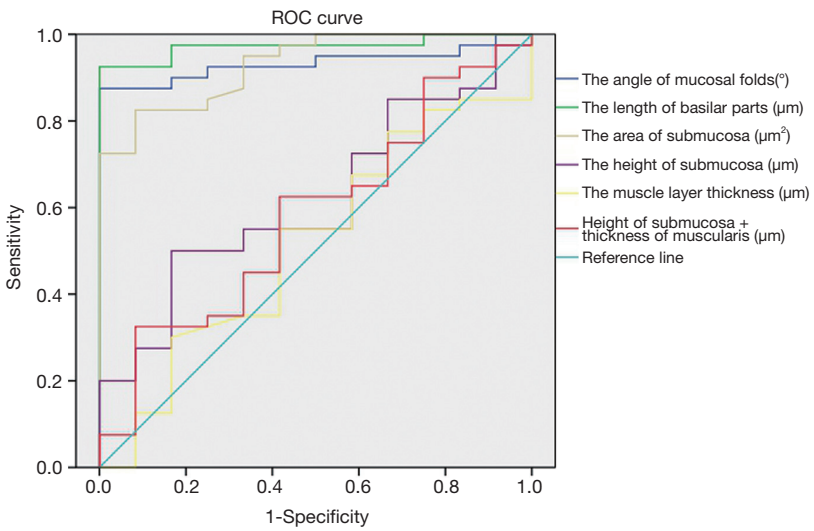

Figure 8 ROC curve of parameters for indexes of colorectal inflammation in HE-stained sections. ROC, receiver operating characteristic.

Table 10 ROC curve of parameters for indexes of colorectal inflammation in OCT images

Parameters for indexes of colorectal inflammation	Area[#]	Standard error	Asymptotic Sig.	Asymptotically 95% confidence interval	
				Lower bound	Upper bound
The length of basilar parts (px)	0.922	0.037	0.000	0.850	0.994
Height of submucosa + thickness of muscularis (px)	0.699	0.085	0.038	0.532	0.866

[#] the area under the ROC curve. OCT, optical coherent tomography; ROC, receiver operating characteristic.

the mucosa to the submucosa (14,21). However, like other structural imaging modalities, the diagnostic relevance of OCT is limited without a robust, quantifiable metric to distinguish control and diseased tissue (22). With the development of portable OCT instruments and other techniques, such as the tethered capsule endoscope (TCE) (23), there is an urgent need for quantitative and qualitative standards of intestinal diseases based on OCT imaging.

Inflammation of colitis in HE sections can be shown as an inflammatory factor infiltration and submucosal edema. Studies have demonstrated the consistency of the

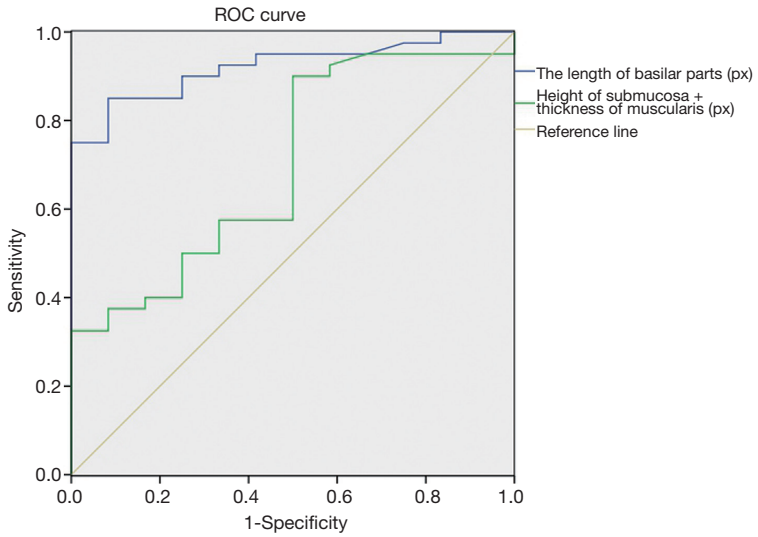

Figure 9 ROC curve of parameters for indexes of colorectal inflammation in OCT images. OCT, optical coherent tomography; ROC, receiver operating characteristic.

morphological stratification of the intestinal walls between OCT imaging and HE-staining. Our study also showed that OCT imaging of the mucosal layer presents as a super-reflective layer, whereas the submucosal and muscular layers are low-reflection layers in the normal mouse colon.

Based on correlations between inflammation and the histological anatomy of the colon, we developed 6 parameters for HE stained sections and 2 for OCT imaging to measure submucosal edema by morphological changes to evaluate the degree of inflammation in the colon.

In the HE-stained sections, the 6 parameters are the angle of mucosal folds, length of basilar parts, area of the submucosa, height of submucosa, thickness of muscularis, and height of submucosa + thickness of muscularis. In OCT imaging, the 2 parameters were the length of basilar parts and the height of submucosa + thickness of muscularis. Four parameters of HE, the angle of mucosal folds, length of basilar parts, submucosal area, and height between submucosal and muscular layers correlated with the degree of inflammation in colitis. Based on the characteristics of OCT scanning, we designed 2 parameters to evaluate inflammation in colitis. Length of basilar part and height of submucosa + thickness of muscularis correlated with the degree of inflammation in colitis. The length of basilar parts (normal group compared with moderate and wild groups) and height of submucosa + thickness of muscularis (wild group compared with other groups) were significantly different between groups and therefore can be used to measure inflammation in colitis.

An interesting finding in this study was that the height of submucosa + thickness of muscularis in OCT images correlated with the degree of inflammation and was a good predictor and index for inflammation. However, it was not statistically significant in HE-stained sections. These results may be due to fact that the OCT scan reflects the visualization of tissue architectural morphology *in situ* and real-time (14,17), whereas there is a dehydration process during the HE-staining, including dewatering. Dehydration in the submucosal layer is more severe than that in the muscular layer, which might have influenced the statistical analysis of the height of submucosa + thickness of muscularis in HE-stained sections. OCT has advantages (*in situ* and real-time analysis) over HE-staining for evaluating the degree of inflammation.

In this study, we induced a mouse model of enteritis and obtained enteritis HE-stained sections. A conventional inflammatory assessment method with HE-staining and 2 parameters (length of basilar parts and height of submucosa + thickness of muscularis) in OCT images were used as indexes for the evaluation of inflammation in colitis. These indexes may have more significance in clinic applications because of the noninvasive and convenient features of OCT scans (14) compared with HE-sections. With the development of portable equipment (24), OCT that includes 2 indexes might be useful for clinical applications. It may be possible to obtain the visualization of sub-surface

tissue morphology *in situ* and real-time in the near future (5,17,20).

Acknowledgments

We thank Sarah Dodds, PhD, from Liwen Bianji, Edanz Editing China (www.liwenbianji.cn/ac), for editing the English text of a draft of this manuscript.
Funding: The study is supported by the Scientific Education Research Fund for Middle-aged and Young Teachers of the Ministry of Fujian province (JK2017021), the Training Fund for Middle-aged and Young Talents of Fujian Province (2017-ZQN-41), the Natural Science Foundation of Fujian Province (2019J01437), the National Natural Science Foundation of China (11601083, U1805263), and Fujian Provincial Science and Technology Project (2019I0004).

Footnote

Conflicts of Interest: All authors have completed the ICMJE uniform disclosure form (available at http://dx.doi.org/10.21037/qims.2020.04.04). The authors have no conflicts of interest to declare.

Ethical Statement: All procedures involving experimental animals were conducted following protocols approved by the Institutional Animal Care and Use Committee (IACUC) of Fujian Medical University.

References

1. Babich JW, Fischman AJ. Targeted imaging of infection. Adv Drug Deliv Rev 1999;37:237-52.
2. Medzhitov R. Origin and physiological roles of inflammation. Nature 2008;454:428-35.
3. Ordás I, Eckmann L, Talamini M, Baumgart DC, Sandborn WJ. Ulcerative colitis. Lancet 2012;380:1606-19.
4. Kaushal P, Somwaru AS, Charabaty A, Levy AD. MR Enterography of Inflammatory Bowel Disease with Endoscopic Correlation. Radiographics 2017;37:116-31.
5. Adler DC, Zhou C, Tsai TH, Schmitt J, Huang Q, Mashimo H, Fujimoto JG. Three-dimensional endomicroscopy of the human colon using optical coherence tomography. Optics Express 2009;17:784-6.
6. Sairenji T, Collins KL, Evans DV. An Update on Inflammatory Bowel Disease. Prim Care 2017;44:673-92.
7. Peyrin-Biroulet L, Panés J, Sandborn WJ, Vermeire S, Danese S, Feagan BG, Colombel JF, Hanauer SB, Rycroft B. Defining Disease Severity in Inflammatory Bowel Diseases: Current and Future Directions. Clin Gastroenterol Hepatol 2016;14:348-354.e17.
8. Camilleri M, Proano M. Advances in the assessment of disease activity in inflammatory bowel disease. Mayo Clin Proc 1989;64:800-7.
9. Soubières AA, Poullis A. Emerging Biomarkers for the Diagnosis and Monitoring of Inflammatory Bowel Diseases. Inflamm Bowel Dis 2016;22:2016-22.
10. Lemmens B, Arijs I, Van Assche G, Sagaert X, Geboes K, Ferrante M, Rutgeerts P, Vermeire S, De Hertogh G. Correlation between the endoscopic and histologic score in assessing the activity of ulcerative colitis. Inflamm Bowel Dis 2013;19:1194-201.
11. Pai RK, Jairath V, Vande Casteele N, Rieder F, Parker CE, Lauwers GY. The emerging role of histologic disease activity assessment in ulcerative colitis. Gastrointest Endosc 2018;88:887-98.
12. Moss AC. The meaning of low-grade inflammation in clinically quiescent inflammatory bowel disease. Curr Opin Gastroenterol 2014;30:365-9.
13. Baars JE, Nuij VJ, Oldenburg B, Kuipers EJ, van der Woude CJ. Majority of patients with inflammatory bowel disease in clinical remission have mucosal inflammation. Inflamm Bowel Dis 2012;18:1634-40.
14. Testoni PA, Mangiavillano B. Optical coherence tomography in detection of dysplasia and cancer of the gastrointestinal tract and bilio-pancreatic ductal system. World J Gastroenterol 2008;14:6444-52.
15. Kawada M, Arihiro A, Mizoguchi E. Insights from advances in research of chemically inducedexperimental models of human inflammatory bowel disease. World J Gastroenterol 2007;13:5581-93.
16. Dieleman LA, Palmen MJ, Akol H, Bloemena E, Peña AS, Meuwissen SG, Van Rees EP. Chronic experimental colitis induced by dextran sulphate sodium (DSS) is characterized by Th1 and Th2 cytokines. Clin Exp Immunol 1998;114:385-91.

17. Fujimoto JG, Pitris C, Boppart SA, Brezinski ME. Optical Coherence Tomography: An Emerging Technology for Biomedical Imaging and Optical Biopsy. Neoplasia 2000;2:9-25.
18. Huang D, Swanson EA, Lin CP, Schuman JS, Stinson WG, Chang W, Hee MR, Flotte T, Gregory K, Puliafito CA. Optical Coherence Tomography. Science 1991;254:1178-81.
19. Drexler W, Morgner U, Ghanta RK, Kärtner FX, Schuman JS, Fujimoto JG. Ultrahigh-resolution ophthalmic optical coherence tomography. Nat Med 2001;7:502-7.
20. Fujimoto JG. Optical coherence tomography for ultrahigh resolution in vivo imaging. Nat Biotechnol 2003;21:1361-7.
21. Tearney GJ, Brezinski ME, Southern JF, Bouma BE, Boppart SA, Fujimoto JG. Optical biopsy in human gastrointestinal tissue using optical coherence tomography. Am J Gastroenterol 1997;92:1800-4.
22. Nair A, Liu CH, Singh M, Das S, Le T, Du Y, Soomro S, Aglyamov S, Mohan C, Larin KV. Assessing colitis ex vivo using optical coherence elastography in a murine model. Quant Imaging Med Surg 2019;9:1429-40.
23. Seibel EJ, Carroll RE, Dominitz JA, Johnston RS, Melville CD, Lee CM, Seitz SM, Kimmey MB. Tethered capsule endoscopy, a low-cost and high-performance alternative technology for the screening of esophageal cancer and Barrett's esophagus. IEEE Trans Biomed Eng 2008;55:1032-42.
24. Li H, Hou X, Lin R, Fan M, Pang S, Jiang L, Liu Q, Fu L. Advanced endoscopic methods in gastrointestinal diseases: a systematic review. Quant Imaging Med Surg 2019;9:905-20.

Cite this article as: Ding J, Lin J, Li Q, Chen X, Chen W, Zhang Q, He S, Wu T, Wang C, Zhong S, Li D. Optical coherent tomography to evaluate the degree of inflammation in a mouse model of colitis. Quant Imaging Med Surg 2020;10(5):945-957. doi: 10.21037/qims.2020.04.04

